INFLUENCE OF METALLURGICAL FACTORS ON HYDROGEN-INDUCED BRITTLE FRACTURE IN AUSTENITIC STAINLESS STEELS

Hannu E. Hänninen and Tero J. Hakkarainen

Technical Research Centre of Finland
SF-02150 Espoo 15, Finland

ABSTRACT

Hydrogen embrittlement (HE) of austenitic stainless steels (AISI 304, AISI 316 and AISI 310) has been studied by charging thin tensile specimens (about 0.1 mm thick) with hydrogen through cathodic polarization and subsequent tensile testing. In thin specimens hydrogen charging can induce an extremely brittle (cleavage) mode of cracking in all studied materials. Fractography shows a clear difference in HE between annealed and cold worked or α'-martensite containing materials. α'-martensite formation enhances the embrittling effect of hydrogen, but cold work as such does not seem to have any deleterious effect. In sensitized materials the transgranular cleavage mode of fracture is replaced by an intergranular mode of fracture. The ductility can be recovered by outgassing of hydrogen. A slow hydrogen-induced crack growth can be produced to some extent when bulk specimens of AISI 316 steel are tested by the slow strain rate method while undergoing cathodic charging.

KEYWORDS

Austenitic stainless steels; hydrogen embrittlement; fractography; plastic deformation; α'-martensite; sensitization.

INTRODUCTION

Cathodic hydrogen charging of thin austenitic stainless steel specimens has been found to reduce severely the ductility and fracture stress of these materials (e.g. Whiteman and Troiano, 1965; Holzworth, 1969; Lagneborg, 1969; Kolts, 1976; Hänninen and Hakkarainen, 1979 and 1980). Recently, a few fractographical studies of this fracture mode have been carried out (e.g. Caskey, 1977; Briant, 1979; Hänninen and Hakkarainen, 1979 and 1980). Only little emphasis has been placed on the role of various metallurgical variables, even though they can also affect the cracking phenomenon (Hänninen, 1979; Thompson and Bernstein, 1980). Of special interest are metallurgical factors like (i) degree of cold work (no α'-martensite formation), (ii) α'-martensite content, (iii) sensitization, and (iv) phosphorus content.

EXPERIMENTAL

The materials used in this study were commercial AISI 304, AISI 316 and AISI 310 stainless steels and an experimental low-P alloy (SCR-1) otherwise corresponding to AISI 304 stainless steel (Table 1). Thin tensile specimens (Fig. 1) were prepared from cold rolled foils (about 0.3 mm thick). The foils were annealed in vacuum for 1 hour at 1373 K and quenched into room temperature water. Cold worked structures were produced by rolling at room temperature, α'-martensite by rolling at 77 K, and sensitized structures by annealing at 923 K. The final thinning was performed by grinding with a 600 grit paper.

Table 1 Chemical Compositions of the Steels.

Material	C	Cr	Ni	Mn	Si	S	P	Cu	Mo
AISI 304	0.07	18.0	8.5	1.44	0.36	0.030	0.016	0.24	0.20
AISI 316	0.03	16.0	10.3	1.43	0.60	0.013	0.030	0.24	2.50
AISI 310	0.08	24.0	19.3	1.30	0.35	-	-	-	0.60
SCR-1	0.08	16.7	10.4	1.40	0.90	-	0.003	-	-

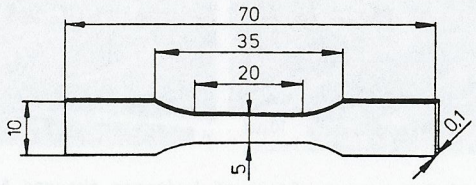

Fig. 1. The thin tensile specimen for cathodic charging tests.

The thin tensile specimens were cathodically charged at 295 K in a 1 N H_2SO_4 solution containing 0.25 g/l of $NaAsO_2$. The current density was 50 mA/cm^2 and a platinum counter electrode was used. The hydrogen charging time was usually 6, but in some cases 24, hours. Increasing the charging time seemed to have no effect on the results. After charging the specimens were tested within 5 min at room temperature in a tensile testing machine at a crosshead speed of about 5 cm/min.

Bulk specimens of AISI 316 steel were studied by using the slow strain rate (SSR) testing method with simultaneous hydrogen charging through cathodic polarization. The specimens had a gauge section 1 mm thick, 10 mm wide and 20 mm long. The strain rate was 3.5×10^{-7} s^{-1} and the solution and the current density as above.

The amount of α'-martensite was measured before and after hydrogen charging by a commercial ferrite detector (Ferritescope).

RESULTS

The results of the tensile tests on reference specimens (without cathodic hydrogen charging) and hydrogen charged solution annealed specimens are shown in Table 2. The effect of metallurgical factors on tensile test results after hydrogen charging is presented in Tables 3 and 4. The tensile test results showed a wide scatter resulting possibly from variations in electrolytic charging

conditions and from difficulties in preparation of reproducible thin tensile specimens. Therefore, only the results of the most brittle specimens are shown in the tables, even though duplicate or triplicate specimens were used for each test.

TABLE 2 Mechanical Properties of the Steels Tensile Tested at Room Temperature before and after Hydrogen Charging.

Material	Reference			Hydrogen charged	
	$R_{p0.2}$, N/mm^2	R_m, N/mm^2	A, o/o	R_m, N/mm^2	A, o/o
AISI 304	310	480	38	210	0
AISI 316	300	480	30	100	0
AISI 310	330	520	25	330	0

TABLE 3 Effect of Plastic Deformation on Fracture Stresses of Hydrogen Charged Specimens.

Material	R_m, N/mm^2	Material	R_m, N/mm^2
AISI 304		AISI 316	
10 o/o deformation	150	10 o/o deformation	430
20 o/o deformation	190	20 o/o deformation	90
30 o/o deformation	250	30 o/o deformation	260
50 o/o deformation	420	50 o/o deformation	260
α'-martensite		AISI 310	
10 o/o	210	10 o/o deformation	480
20 o/o	70	30 o/o deformation	400
		50 o/o deformation	460

Fracture surfaces of the hydrogen charged materials are shown in Figs. 2-6. Figure 2 shows typical features of brittle cracking. A common feature for the cracking of all steels is the formation of crystallographic saw-tooth profiles in the steps between flat parallel facets. Another typical feature in these experiments was a narrow zone of ductile dimpled fracture surface in the middle of most specimens. The ductile zone was widest in the AISI 310 steel specimens, which also showed higher fracture stresses than the other materials. Comparing duplicate specimens, it was found generally that the fracture stress increased with increasing amounts of ductile fracture. The ductility, however, is localized into the crack tips of the hydrogen-induced brittle cracks starting from the surfaces on both sides of the specimen, and cannot usually be observed on the stress strain curves.

TABLE 4 Effect of Sensitization on Fracture Stresses of Hydrogen Charged Specimens.

Material	R_m, N/mm^2	Material	R_m, N/mm^2
AISI 304		AISI 310	
1h/923 K	310	24h/923 K	400
10h/923 K	230	50h/923 K	550
AISI 316			
24h/923 K	240		

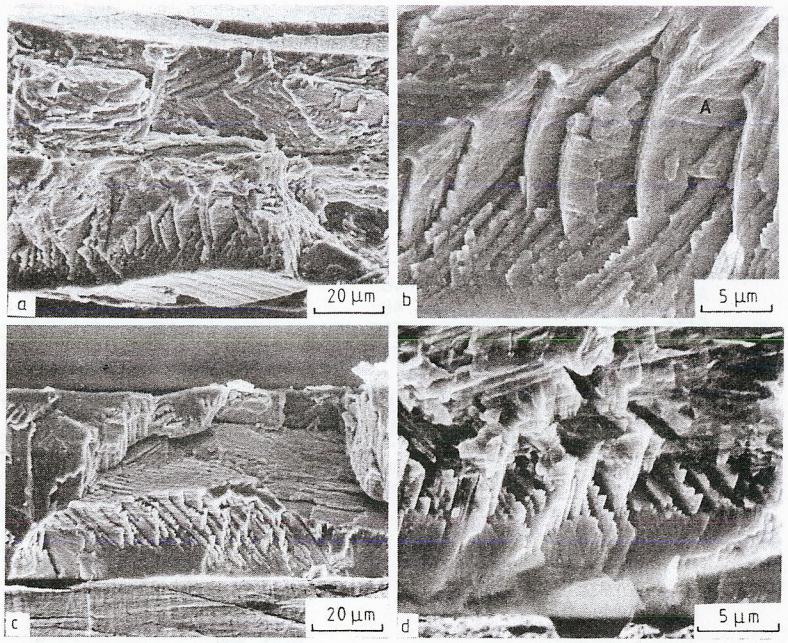

Fig. 2. Examples of fracture surfaces of hydrogen charged austenitic stainless steels. (a) AISI 304. (b) Detail of (a). Note the slip steps at A. (c) AISI 316. Note the variability in the morphology of brittle cracking. (d) AISI 310, a detail of the brittle zone near the outer surface. Note the formation of slip steps on the brittle fracture surface and change in fracture surface morphology deeper in the specimen.

In AISI 304 stainless steel, increasing cold work to over 20 o/o increased the amount of ductile dimpled fracture surface. In 50 o/o cold worked materials only small brittle hydrogen-induced surface cracks were detected (Fig. 3b). The same trend was found in the case of other studied steels. When α'-martensite was produced intentionally before hydrogen charging, the fracture morphology changed into a quasi-cleavage (Fig. 3c), typical of quenched and tempered steels. The fracture surface in this case consists of small facets. Also in specimens with α'-martensite, a ductile dimpled (very flat) fracture was found (Fig. 3d), but to lesser extent.

Sensitization heat treatments change the mostly transgranular hydrogen-induced cracking of solution annealed steels into an intergranular mode of cracking (Fig. 4). This change was not found to cause marked changes in tensile test results. In the AISI 310 steel the depth of hydrogen-induced brittle cracks increased, and extended in some parts across the specimens. The crack path seemed to be along the grain boundary or along the phase boundary between carbide and the matrix.

The low-P-containing 18/10-steel was also found to be susceptible to hydrogen-induced cracking (fracture stress 340 N/mm^2). The morphology of cracking does not markedly differ from that of commercial alloys with higher phosphorus content (Fig. 5).

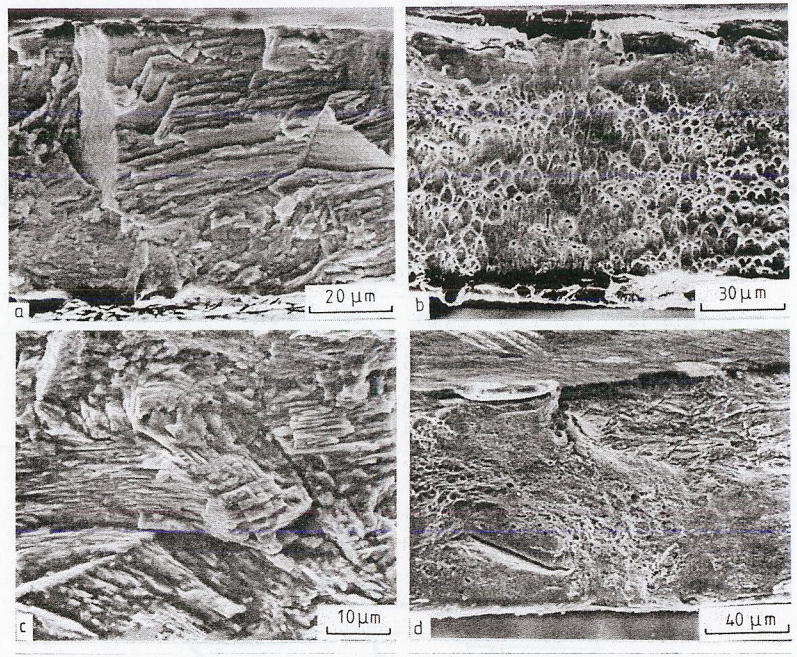

Fig. 3. Examples of fracture surfaces of hydrogen charged AISI 304 steel cold worked before hydrogen charging. (a) 20 o/o deformed (no α'-martensite). The mode of cracking is similar to that of the solution annealed condition. (b) 50 o/o deformed (α'-martensite content 2.4 o/o). Mainly dimpled cracking. (c) 12 o/o α'-martensite. Quasi-cleavage type of cracking. (d) 12 o/o α'-martensite. Partly ductile dimpled fracture.

In SSR tests shallow surface cracks were formed. The surface cracks did not, however, have a detectable effect on the general ductility of the specimens. In Fig. 6a, a general view of a hydrogen-induced crack (less than 1 mm deep) starting from the edge of a specimen is shown. This specimen cracked after 16 days when the tensile stress was about 600 N/mm^2 and elongation about 45 o/o . Final fracture occured by ductile manner when the largest of the edge cracks turned into ductile tear. The detailed hydrogen-induced fracture surface morphology (Fig. 6b) corresponds to that obtained in cold worked thin tensile specimens.

Outgassing of hydrogen was studied both at room temperature and at elevated temperatures. At room temperature the ductility started to recover after one week ageing. The recovery was faster at elevated temperatures. Small surface cracks were always observed after tensile testing the aged specimens.

Measurements to detect the possible hydrogen-induced α'-martensite were made on the surfaces of the specimens, as near the main crack as possible, using a ferrite detector. No evidence of α'-martensite was found in annealed specimens. When the α'-martensite content was measured after tensile testing of the deformed specimens, generally slightly smaller values were obtained than before testing. This was thought to be due to the shallow surface cracks formed during testing.

The microstructure of the tensile specimens was also studied by transmission electron microscopy after tensile testing. These results are reported in detail elsewhere (Hänninen, Hakkarainen and Nenonen, 1980). No phase transformations were observed.

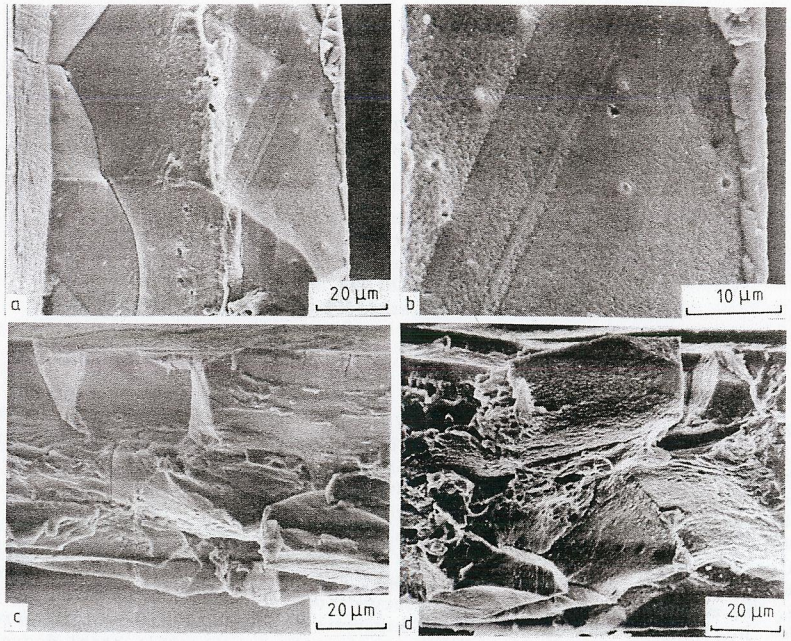

Fig. 4. Examples of fracture surfaces in sensitized steels after hydrogen charging. (a) AISI 304 steel (sensitized 24h/923 K). Note the narrow ductile zone in the middle of the fracture surface. (b) Detail of (a). (c) AISI 316 steel (sensitized 24h/923 K). (d) AISI 310 steel (sensitized 50h/923 K).

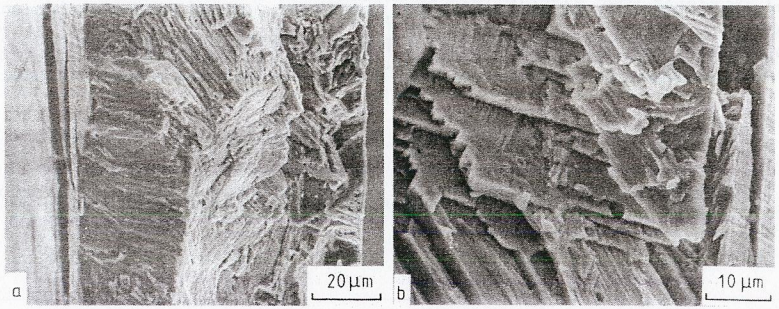

Fig. 5. Hydrogen-induced cracking of the low-P-containing (0.003 o/o P) 18/10-steel. Note that the brittle cracking extends through the specimen.

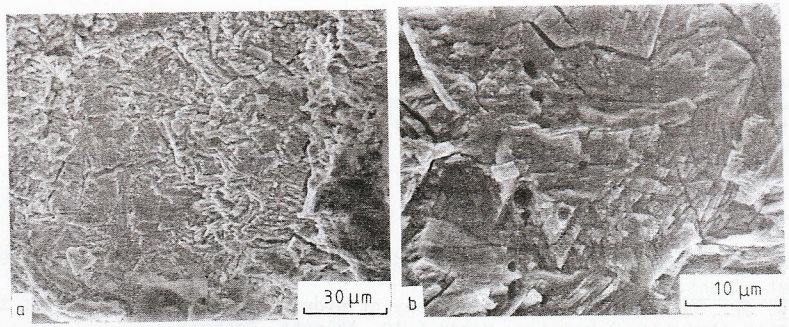

Fig. 6. Fracture surface of the SSR tested AISI 316 steel. (a) A crack initiated at the edge of the specimen. (b) A detail of the hydrogen-induced crack. Note the crystallographic details and secondary microcracks.

DISCUSSION

A loss of ductility in the surface layers of all austenitic stainless steels studied can be observed after cathodic charging with hydrogen. By using sufficiently thin specimens (about 0.1 mm thick) the materials can be even fully embrittled. The loss of ductility after hydrogen charging can be recovered by outgassing of hydrogen. After outgassing, however, shallow surface cracking is observed. These cracks are thought to form when the hydrogen expanded lattice shrinks during the outgassing, and a tensile strain is developed at the surface, because the diffusion of hydrogen in austenite is slow.

Increasing the dislocation density of the steels by extensive plastic deformation seems to make the microstructure less susceptible for a hydrogen-induced cleavage-like fracture. Instead, dimpled ductile fracture is favoured. This behaviour may be explained by trapping of hydrogen to dislocations and the difficulty of hydrogen-induced cleavage crack propagation in a structure of high dislocation density.

The change of the brittle cleavage-like fracture morphology to quasi-cleavage, if sufficiently α'-martensite is present, indicates that in this case the fracture propagates along the pre-existing α'-martensite. The decreasing amount of dimpled fracture in α'-martensite containing specimens suggests that α'-martensite facilitates the diffusion of hydrogen into the steel.

Sensitization seems both to facilitate the penetration of hydrogen along the grain boundaries into the steels and to introduce susceptibility to brittle fracture along grain boundaries.

The similar behaviour of the two 18/10-steels with different phosphorus contents indicates that the impurities like phosphorus do not determine the hydrogen embrittlement of austenite.

The fact that no α'-martensite could be detected with a ferrite detector in the solution annealed specimens after hydrogen charging and tensile testing are in accordance with transmission electron microscope observations from the tensile specimens (Hänninen, Hakkarainen and Nenonen, 1980), where neither α'- nor ε-martensite were found. This does not prove yet, of course, that there could not be narrow zones of martensite along the fracture surfaces or in the surface layers of the specimens.

ACKNOWLEDGEMENT

The authors acknowledge Prof. J. Forstén for his valuable advice and comments. This work was supported in part under Reactor Materials Research Project at the Technical Research Centre of Finland and financed by the Ministry of Trade and Industry in Finland.

REFERENCES

Briant, C. L. (1979). Hydrogen assisted cracking of type 304 stainless steel. Met. Trans., 10A, 181-189.

Caskey, Jr., G. R. (1977). Fractography of hydrogen-embrittled stainless steel. 106th AIME Annual Meeting, March 6-10, Atlanta, Georgia.

Holzworth, M. L. (1969). Hydrogen embrittlement of type 304L stainless steel. Corrosion, 25, 107-115.

Hänninen, H. E. (1979). Influence of metallurgical variables on environment-sensitive cracking of austenitic alloys. Int. Met. Rev., 24, 85-135.

Hänninen, H., and T. Hakkarainen (1979). Fractographic characteristics of a hydrogen-charged AISI 316 type austenitic stainless steel. Met. Trans., 10A, 1196-1199.

Hänninen, H., and T. Hakkarainen (1980). On the effects of α'-martensite in hydrogen embrittlement of a cathodically charged AISI type 304 austenitic stainless steel. Corrosion, 36, 47-51.

Hänninen, H., T. Hakkarainen, and P. Nenonen (1980). To be published.

Kolts, J. (1976). Hydrogen induced delayed failure of type 310 stainless steel foils. Stress Corrosion - New Approaches, ASTM STP 610. ASTM, Pennsylvania, pp. 366-380.

Lagneborg, R. (1969). Hydrogen embrittlement in austenitic steels and nickel-base alloys. JISI, 207, 363-366.

Thompson, A. W., and I. M. Bernstein (1980). The role of metallurgical variables in hydrogen-assisted environmental fracture. In M. G. Fontana and R. W. Staehle (Ed.), Advances in Corrosion Science and Technology, Vol. 7, Plenum Publishing Corporation, New York, pp. 53-175.

Whiteman, M. B., and A. R. Troiano (1965). Hydrogen embrittlement of austenitic stainless steel. Corrosion, 21, 53-56.